PHILIPPINE ENGINEERING JOURNAL
PEJ 2004; **Vol. 25 No. 2**:53–72

On the Use of Entropic Regularization for Identification of Cohesive Crack Parameters

Norbert S. Que*

Department of Engineering Sciences
University of the Philippines Diliman
Quezon City 1101 PHILIPPINES

ABSTRACT

The fracture parameters governing the cohesive crack model is obtained through the use of entropic regularization. Specifically, it is employed as a smoothing technique that lends to the solution of a difficult identification problem cast as a mathematical program with equilibrium constraints (MPEC). Results suggest that reformulation of MPEC as a nonlinear programming problem using entropic regularization show promise in the solution of the parameter identification problems considered in this paper.

1. INTRODUCTION

Research has shown that the application of the concepts of fracture mechanics can lead to satisfactory simulation and prediction of the local damage phenomena and the effect of structural size to fracture (Bažant and Planas, [4]). Moreover, it offers a logical approach to structural analysis and design based on sound mathematical and mechanics concept.

The applicability of fracture mechanics to real engineering problems depends on the knowledge of fracture models that can be used to satisfactorily simulate the behavior of quasibrittle fracture. One such model is the Cohesive Crack Model (CCM) the main idea of which was developed independently by Dugdale [19] and Barenblatt [3]. The formulation of the CCM as a suitable nonlinear model for mode I fracture, however, is largely credited to the work carried out by Hillerborg and his co-workers [24].

Like all fracture models, the CCM is governed by a tension-softening relation that describes the fracture behavior of a quasibrittle material. Its application to fracture mechanics requires the characterization of the softening law, where, in most instances, the shape of the softening law is known *a priori*. Even with a simplified softening relation, such as the one-branch law used by Hillerborg and co-workers [24], the identification of the parameters characterizing the relation is not a trivial task.

The advancement of experimental techniques makes it possible to characterize some of the fracture properties of cementitious materials. The uniaxial tensile test, for instance, is

*Correspondence to: Department of Engineering Sciences, 304 Melchor Hall, Quezon City 1101, Philippines

Received July 1, 2005
Revised February 22,2006
Accepted February 24,2006

universally accepted as the most direct way of doing this. Experimentalists (Petersson, [32]; Reinhardt, *et al.*, [36]; Cattaneo and Rosati, [11]; van Mier and van Vliet, [43]) generally agree, however, that this type of mechanical testing is difficult to perform due in part to the inability to consistently obtain uniform stress distributions across the crack. This could be attributed to specimen imperfections and accidental eccentricity of the loading apparatus. Moreover, a study conducted by Hordijk *et al.* [25] cast doubt on the reliability of the results obtained in the uniaxial tensile test.

A number of indirect approaches that rely on optimization procedures to obtain the cohesive fracture parameters of predefined softening laws have been introduced in various literatures. Among these include the works of Roelfstra and Wittmann [38], Ulfkjær and Brincker [42], Mihashi and Nomura [30], Bolzon and Maier [6], Que and Tin-Loi [40], Tin-Loi and Que [39].

The methodology proposed by Tin-Loi and Que [39] will be adopted in this work. The formulation of the parameter identification problem is cast as a special type of constrained optimization problem known in the mathematical programming literature as a mathematical program with equilibrium constraints or MPEC where equilibrium constraints refer to complementarity conditions involving the orthogonality of two sign-constrained vectors. A direct solution to MPEC is known to be very difficult (Luo *et al.*, [28]). To overcome this difficulty, MPEC is reformulated as a nonlinear programming problem (NLP).

The main objective of this paper is to show that a smoothing function based on entropic regularization (Fang and Wu, [20]) can be used as an NLP-based algorithm to solve a parameter identification problem cast as an MPEC. Identification is carried out using actual experimental data obtained from three-point bend test and wedge splitting test using two-branch and three-branch laws to simulate the fracture behavior of the materials.

This paper is organized as follows. In Section 2, key components of the CCM are discussed. The complementarity formulation of the two-branch and three-branch softening laws are described. The discretization of a structural model using the boundary element procedure is presented. The formulation of the direct problem as a mixed complementarity problem is explained. Section 3 deals with the formulation of the inverse problem where the identification problem is cast as MPEC. Section 4 introduces a solution to the MPEC by reformulating the identification problem as NLP using smoothing algorithm based on entropic regularization. The method is tested using several experimental data sets. The paper concludes in Section 5.

2. FORMULATION OF THE DIRECT PROBLEM

A fundamental assumption that characterizes the CCM from other fracture models is the idea that inelastic deformation and micro-cracking occur in a narrow area, called the fracture process zone. The localization of the damage zone allows the interpretation of the fracture process zone as a line crack of zero width. This further permits the assumption that the bulk material remains elastic and isotropic. The variation of the tensile stress and displacement discontinuity along the length of the fracture process zone can be described conveniently by a softening law. Figure 1 illustrates the key idea of the CCM and the associated softening relation, in this case, a nonlinear softening law for mode I fracture.

As shown in the Figure 1, the distribution of tensile stress varies nonlinearly along the length of the fracture process zone. At the tip of the fracture process zone, the stress and deformation are equal to the tensile strength of the material and zero, respectively. It is assumed that

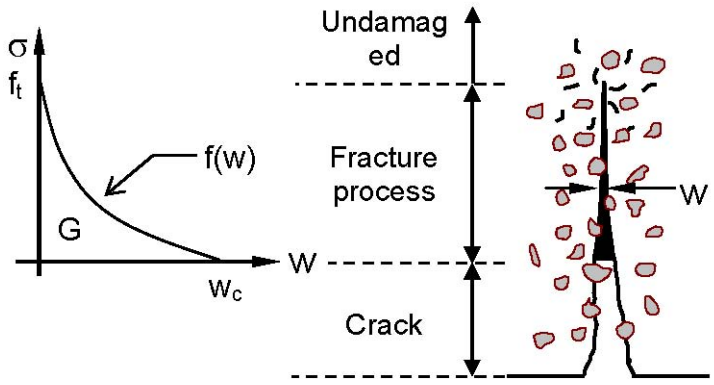

Figure 1. Definition of the cohesive crack model.

fracture initiates when the principal stress at a point attains the value of the tensile strength f_t of the material. Crack propagates orthogonal to the direction of the principal stress. As Hillerborg *et al.* [24] have pointed out, this is not a real crack but only a fictitious one which is capable of transferring stresses between crack faces, thus the so-called "fictitious crack model".

The model is a convenient mathematical idealization of the material damage occurring in the fracture process zone of quasibrittle materials. The stress on the crack interface decreases with increasing displacement discontinuity w. In the model, a true crack appears when the critical crack width w_c is reached. At this point, the value of the tensile stress drops to zero.

An essential ingredient of the cohesive crack model is the softening relation or softening law (see Figure 1). The softening law is the analytical description of the variation of the tensile stress and displacement discontinuity w along the length of the fracture process zone. For as long as tension forces dominate in a structure and where the effects of lateral deformations and stresses can be neglected, the softening law is considered a material property.

The problem of characterizing the softening law is an important component in the use of the CCM for fracture analysis. Considerable research has been spent towards its determination using direct (experimental) and indirect methods (inverse analysis and other techniques). Practical applications of the model often call for simplified softening relations to be employed. For instance, the use of a two-branch law (Petersson, [32]) is extensively reported in literatures and is generally considered a good approximation of the mode I fracture behaviour of concrete. Nonlinear softening laws have also been used in the investigation of the fracture processes of cementitious materials (Foote *et al.*, [21]; Planas and Elices, [33]; Hu and Mai, [26]; Carpinteri and Massabò, [10]; Reinhardt and Xu, [37]. The softening curves mentioned can satisfy the modelling requirement for computational simplicity and predictive accuracy.

Depending on the chosen softening relation, as few as two parameters may be required to completely describe the softening law. For example, a generic nonlinear softening curve (Figure 1) with a known softening function $\sigma = f(w)$ requires only two parameters (e.g., f_t and w_c or f_t and G_F) to completely describe the relation. In the context of the CCM, these

parameters are considered material properties which are independent of specimen geometry and loading. Often than not, however, only the tensile strength f_t and the fracture energy G_F are chosen due to the difficulty of experimentally measuring the critical crack width w_c. Both the tensile strength f_t and the fracture energy G_F can be determined by performing appropriate fracture mechanics tests. It is worth mentioning that in some engineering applications, it may not even be necessary to completely characterize the softening law. For instance, if only the maximum load of a structure is required for design purposes, then the tensile strength f_t and the initial slope of the softening curve will provide sufficient information (Alvaredo and Torrent, [1]; Guinea *et al.*, [23]). In this paper, two-branch and three-branch piecewise linear softening laws are used in characterizing the cohesive fracture properties of quasibrittle materials.

The analytic description of a piecewise linear softening law in complementarity format was first developed by Bolzon *et al.* [7] using unilateral contact and nonlinear softening spring analogy. However, due to the use of pseudo slope in the formulation, the geometrical representation of the parameters is difficult to visualize. Also, the formulation limits the general configuration of the softening curve to a "convex" one. Although the behaviour of a majority of quasibrittle materials can be approximated well using convex-shaped piecewise linear laws, there may be cases, especially for new materials, when Dugdale-type (concave shape) curves or convex-concave shaped linear laws yield better solutions.

Tin-Loi and Xia [41], in the context of softening of struts, have proposed an alternative complementarity formulation for a piecewise linear hardening-softening relation which overcomes the abovementioned limitations. The resulting relation is a general and powerful description of piecewise linearized laws. In the formulation, actual softening slopes are used and "concave-convex" representation of a softening curve is accommodated.

Using the formulation proposed by Tin-Loi and Xia [41], the analytic description of a two-branch softening law, as shown in Figure 2, is expressed as:

$$\mathbf{f}^i = t_b \mathbf{v}_1^i + t_c \mathbf{v}_2^i + \left(h_1 \mathbf{M}_1^i + h_2 \mathbf{M}_2^i\right) \mathbf{z}^i + t^i \mathbf{n}^i, \tag{1}$$

$$\mathbf{f}^i \geq \mathbf{0}; \quad \mathbf{z}^i \geq \mathbf{0}; \quad \mathbf{f}^{iT} \mathbf{z}^i = 0, \tag{2}$$

where subscript i indicates pointwise application of the expressions along the crack locus and $t^i$is the normal traction at location i. $\mathbf{f}^i \in \Re^3$ is a non-negative auxiliary vector (which can be interpreted, in the spirit of classical plasticity, as yield or activation function). $\mathbf{z}^i \in \Re^3$ is another non-negative auxiliary vector, which represents opening displacements.

The vector of yield functions is given by $\mathbf{f}^{iT} = \begin{bmatrix} f_1^i & f_2^i & f_3^i \end{bmatrix}$ and the vector of opening displacements by $\mathbf{z}^{iT} = \begin{bmatrix} z_1^i & z_2^i & z_3^i \end{bmatrix}$. It must be noted that under this definition, f_1^i, f_2^i and f_3^i are the activation functions of the third, first and second softening branches respectively, and $z_1^i = w$ represents the final opening displacement of point i in the crack locus. Vectors of constant entries are written as

$$\mathbf{v}_1^i = \begin{bmatrix} 0 \\ -1 \\ 1 \end{bmatrix}, \quad \mathbf{v}_2^i = \begin{bmatrix} 1 \\ 1 \\ 0 \end{bmatrix}, \quad \mathbf{n}^i = \begin{bmatrix} -1 \\ 0 \\ 0 \end{bmatrix},$$

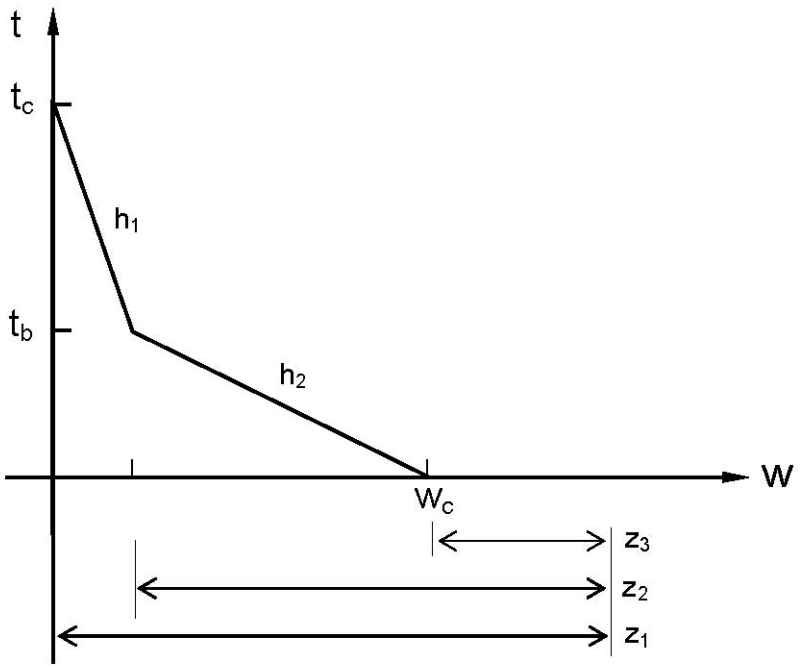

Figure 2. Definition a of two-branch softening law using actual slopes.

and the matrices $\mathbf{M}_1^i$ and $\mathbf{M}_2^i$ are expressed as

$$\mathbf{M}_1^i = \begin{bmatrix} -1 & 1 & 0 \\ -1 & 1 & 0 \\ 0 & 0 & 0 \end{bmatrix}, \quad \mathbf{M}_2^i = \begin{bmatrix} 0 & -1 & 1 \\ 0 & 0 & 0 \\ 0 & -1 & 1 \end{bmatrix}$$

The relation set expressed by Equation (2) is referred to in the mathematical programming literature (Cottle *et al.*, [15]) as a Linear Complementarity Problem (LCP). The relation fully describes the characteristics of the piecewise linear softening law shown in Figure 2. For instance, it is easy to verify that for any given traction $0 \leq t \leq t_c$ precisely two solutions exist for w, one corresponding to the elastic case $w = 0$ (vertical branch) and the other due to activation of the softening mode. Likewise, for any given crack width $0 \leq w \leq w_c$, there exists only one solution to the LCP.

As shown in the Figure, four parameters are required to completely characterize a two-branch softening curve, namely the tensile strength t_c, the breakpoint strength t_b, the slope of the first and second softening branches, h_1 and h_2, respectively.

The analytic description of a three-branch softening law is derived in the same manner as

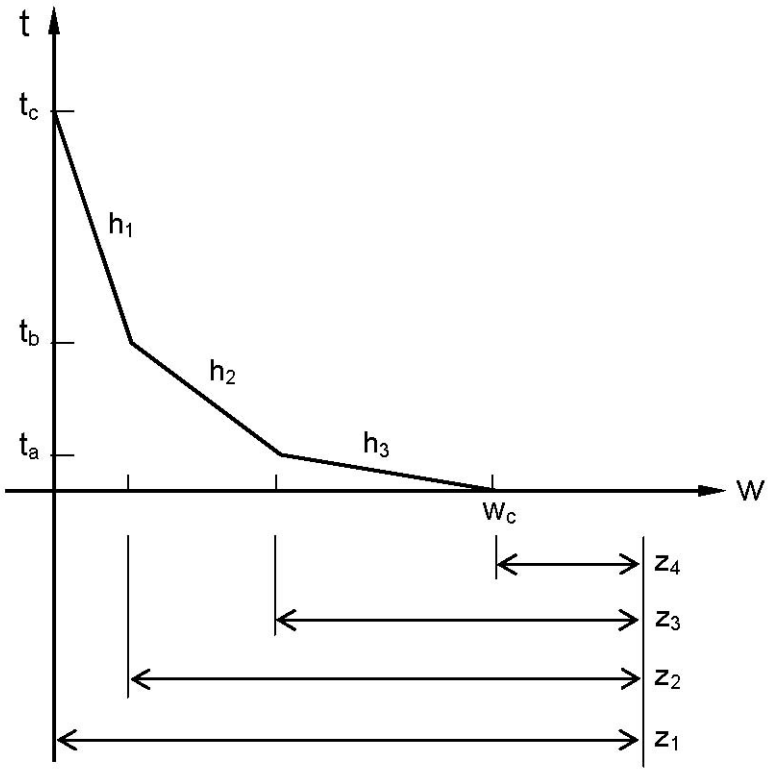

Figure 3. Definition a of three-branch softening law using actual slopes.

that of the two-branch law. Referring to Figure 3, the LCP formulation is expressed as:

$$\mathbf{f}^i = t_a \mathbf{v}_1^i + t_b \mathbf{v}_2^i + t_c \mathbf{v}_3^i + \left(h_1 \mathbf{M}_1^i + h_2 \mathbf{M}_2^i + h_3 \mathbf{M}_3^i\right) \mathbf{z}^i + t^i \mathbf{n}^i, \tag{3}$$

$$\mathbf{f}^i \geq \mathbf{0}; \quad \mathbf{z}^i \geq \mathbf{0}; \quad \mathbf{f}^{iT} \mathbf{z}^i = 0, \tag{4}$$

where h_1, h_2 and h_3 are the slopes of the first, second and third softening branches respectively, t_c is the tensile strength, t_a and t_b are the breakpoint strengths. These comprise the parameters required of the three-branch softening law. The vectors of yield functions $\mathbf{f}^i \in \Re^4$ and opening displacements $\mathbf{z}^i \in \Re^4$ are defined as $\mathbf{f}^{iT} = \begin{bmatrix} f_1^i & f_2^i & f_3^i \end{bmatrix}$ and $\mathbf{z}^{iT} = \begin{bmatrix} z_1^i & z_2^i & z_3^i \end{bmatrix}$, respectively. As in the case of the two-branch law, f_1^i represents the yield function of the horizontal branch and f_2^i, f_3^i and f_4^i are the yield functions of the first, second and third softening branches, respectively. Also, $z_1^i = w$ represents the final opening displacement of the ith point in the crack locus.

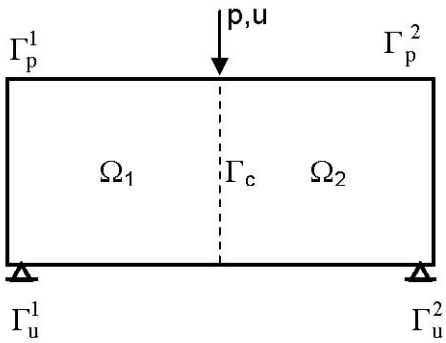

Figure 4. Problem definition for mode I fracture.

The vectors of constant entries are given by

$$\mathbf{v}_1^i = \begin{bmatrix} 0 \\ 0 \\ -1 \\ 1 \end{bmatrix}, \quad \mathbf{v}_2^i = \begin{bmatrix} 0 \\ -1 \\ 1 \\ 0 \end{bmatrix}, \quad \mathbf{v}_3^i = \begin{bmatrix} 1 \\ 1 \\ 0 \\ 0 \end{bmatrix}, \quad \mathbf{n}^i = \begin{bmatrix} -1 \\ 0 \\ 0 \\ 0 \end{bmatrix},$$

while the matrices are written as

$$\mathbf{M}_1^i = \begin{bmatrix} -1 & 1 & 0 & 0 \\ -1 & 1 & 0 & 0 \\ 0 & 0 & 0 & 0 \\ 0 & 0 & 0 & 0 \end{bmatrix}, \quad \mathbf{M}_2^i = \begin{bmatrix} 0 & -1 & 1 & 0 \\ 0 & 0 & 0 & 0 \\ 0 & -1 & 1 & 0 \\ 0 & 0 & 0 & 0 \end{bmatrix}, \quad \mathbf{M}_3^i = \begin{bmatrix} 0 & 0 & -1 & 1 \\ 0 & 0 & 0 & 0 \\ 0 & 0 & 0 & 0 \\ 0 & 0 & -1 & 1 \end{bmatrix}$$

To provide a generic description of the fracture problem at hand, consider a typical three-point bend test as shown in Figure 4. Due to the symmetry of geometry and loading, mode I fracture is expected. For this reason, the location of the potential crack discontinuities Γ_c is known *a priori* and coincides with the axis of symmetry of the structure.

In accordance with the cohesive crack model, all nonlinearities are assumed to be concentrated along the locus of discontinuities Γ_c for which crack is expected to propagate. The potential crack path Γ_c divides the specimen into two homogeneous zones, Ω_1 and Ω_2, which are assumed to be linear elastic and isotropic. Each zone is bounded by the potential crack surface Γ_c, the constrained surface Γ_u and the unconstrained surface Γ_p As is usual in structural modeling, displacements are prescribed in the constrained surface Γ_u while external actions are imposed in the unconstrained surface Γ_p.

The abovementioned assumptions make it possible to express the nonlinear response of the structure as being governed by the following integral equation (Cen and Maier, [12]; Maier and Frangi, [29]):

$$t(x) = \int_{\Gamma_c} Z(x,s)\, w(s)\, d\Gamma + t^e(x), \quad x, s \in \Gamma_c \tag{5}$$

where the normal tractions t on the interface Γ_c are given by the superposition of the effects of the elastic and inelastic actions. The latter is due to actual normal displacement discontinuities w while the former is from an external action (in the case of a stable three-point bend test, is an imposed displacement u) in the absence of kinematic discontinuities. The first term on the right hand side of Equation (5) represents the inelastic effect and is described through Green's function or influence coefficients $Z(x,s), x, s \in \Gamma_c$ ($x \equiv$ field point,$s \equiv$ source point). These influence coefficients can be determined from an elastic analysis of the structure as the normal tractions t due to unit normal displacement discontinuities w across Γ_c in the unloaded structure. The second term on the right hand side of Equation (5) refers to the elastic response of the uncracked structure for a given controlled displacement u.

In most practical cases, the analytical expressions for $Z(x,s)$ may not be possible to determine. Hence, for purposes of numerical analysis, a space discretization of Equation (5) is required. This can be achieved by employing any numerical analysis techniques where the finite element and boundary element approaches are eminently applicable. However, since only the variables lying at the interface Γ_c are to be determined a multizone BEM approach can be used to advantage over the more traditional FEM.

The idea of a multizone BEM for fracture analysis is to introduce distinct zones (see Figure 4), each one containing the crack surface, formulated by its own system of boundary integral equations. The zones are joined together by enforcing compatibility and equilibrium conditions at the crack interface. The paper by Tin-Loi and Que [39] provides useful information in the implementation of a multizone BEM for fracture problems.

Discretization of the structure using multizone BEM and enforcing compatibility and equilibrium conditions at the crack interface lead to the following expression for the traction

$$\mathbf{t} = \mathbf{t}^e + \mathbf{Z}\mathbf{w} \tag{6}$$

where $\mathbf{t}$ is a vector of normal tractions, $\mathbf{t}^e$ is a vector of elastic tractions due to externally applied actions on the structural model, $\mathbf{Z}$ (discretized version of Green's function) is a square matrix of influence coefficients and $\mathbf{w}$ is a vector of displacement discontinuity. From the same formulation of the computational model, the load "reaction" p as shown in Figure 4 due to an imposed displacement u is obtained as

$$p = p^e + \mathbf{r}\mathbf{w} \tag{7}$$

where p^e is the elastic response corresponding to u, and $\mathbf{r}$ is a known vector obtainable from the computational model.

In the case of the two-branch law, collecting relations (1), (2) and (6) for all points i on the interface leads to the following mixed complementarity problem (MCP)

$$\mathbf{t} = \mathbf{t}^e + \mathbf{Z}\mathbf{w}$$

$$\mathbf{f} = t_b\mathbf{v}_1 + t_c\mathbf{v}_2 + (h_1\mathbf{M}_1 + h_2\mathbf{M}_2)\,\mathbf{z} + \mathbf{N}\mathbf{t} \tag{8}$$

$$\mathbf{f} \geq \mathbf{0}, \quad \mathbf{z} \geq \mathbf{0}, \quad \mathbf{f}^T\mathbf{z} = 0$$

A solution of the MCP (8) is achieved when the displacement discontinuity and traction vectors are determined given the softening parameters t_b, t_c, h_1 and h_2. Once a solution is found, Equation (7) can then be used to obtain the load-displacement $(p-u)$ diagram of the structure.

3. INVERSE ANALYSIS

Conceptually, the parameter identification problem is easy to understand and follows the traditional methodology underlying classical fitting problems. Its formulation is straightforward and involves some error norm and appropriate constraints. Numerically, however, the particular problem that needs to be solved is highly challenging, primarily because some constraints in the formulation involve complementarity conditions.

The parameter identification problem can be formulated as follows. Start with the assumption that a number of pairs of load-displacement readings $\left(p_j^m, u_j^m\right)$ has been obtained where $j \in \mathbf{J}$ represents a measurement with $\mathbf{J}$ denoting the set of all measurements; a superscript m indicates a measured quantity. Readings $\left(p_j^m, u_j^m\right)$ usually represent actual experimental data obtained from mode I stable fracture tests (or a pseudo-data generated from a forward analysis using Equations (7) and (8) of the fracture problem). Let $\left(p_j^c, u_j^c\right)$ denote, respectively, the reaction and displacement values that would be computed (hence the superscript c) from the numerical model.

After this step, set up a suitable objective function (error norm) ω, defined as some norm of the difference between measured reactions p_j^m and computed reactions p_j^c. The objective function provides a measure of the "goodness" of the results obtained from the numerical model. It must be noted that, if desired, statistical characterisations of experimental errors can be accounted for by appropriately weighting the objective function (Bolzon *et al.*, [8]; Bolzon and Maier, [6]). The fracture parameters are determined by minimising ω subject to constraints of the form given by Equations (2) or (4) and (7) and other constraints which may help in the convergence of the optimization process. The parameter identification problem can be stated formally as the following constrained optimization problem:

$$
\begin{aligned}
\min_{\forall j \in \mathbf{J}} \quad & \omega \equiv \sum_j \left\| p_j^m - p_j^c \right\| \\
\textit{subject to} \quad & \mathbf{t}_j = \mathbf{Z}\mathbf{w}_j + \mathbf{t}_j^e, \\
& \mathbf{f}_j \geq \mathbf{0}, \quad \mathbf{z}_j \geq \mathbf{0}, \quad \mathbf{f}_j^T \mathbf{z}_j = 0, \\
& p_j^c = p_j^e + \mathbf{r}^T \mathbf{w}_j, \\
& \textit{other constraints}
\end{aligned}
\tag{9}
$$

where $\|\cdot\|$ indicates some error norm. Tin-Loi and Que [39] investigated the suitability of various types of error norms for the parameter identification problem given in Equation (9). The study indicates the robustness of the 1-norm and it will employed in this work.

For a two-branch softening law, the constrained optimization formulation is expressed as

$$
\begin{aligned}
\min_{\forall j \in \mathbf{J}} \quad & \omega \equiv \sum_j \left\| p_j^m - p_j^c \right\| \\
\textit{subject to} \quad & \mathbf{t}_j = \mathbf{Z}\mathbf{w}_j + \mathbf{t}_j^e, \\
& \mathbf{f}_j = t_b \mathbf{v}_1 + t_c \mathbf{v}_2 + \left(h_1 \mathbf{M}_1 + h_2 \mathbf{M}_2\right) \mathbf{z}_j + \mathbf{N}\mathbf{t}_j, \\
& \mathbf{f}_j \geq \mathbf{0}, \quad \mathbf{z}_j \geq \mathbf{0}, \quad \mathbf{f}_j^T \mathbf{z}_j = 0, \\
& p_j^c = p_j^e + \mathbf{r}^T \mathbf{w}_j, \\
& t_c \geq t_b, \\
& \textit{bounds on } (t_b, t_c, h_1, h_2)
\end{aligned}
\tag{10}
$$

As shown in relations (10), one constraint imposed for the two-branch optimisation formulation is that the tensile strength t_c is greater than or equal to the breakpoint strength t_b of the softening curve (see Figure 2). Such a simple (and obvious) expression usually helps in the optimisation procedure. Other constraints include imposed bounds on the parameters. It must be noted that these bounds, i.e., upper and lower bounds, are usually prescribed by the analyst based on an engineering knowledge of the material.

For a three-branch law, the formulation for the identification problem is

$$
\begin{aligned}
\min_{\forall j \in \mathbf{J}} \quad & \omega \equiv \sum_j \left\| p_j^m - p_j^c \right\| \\
\textit{subject to} \quad & \mathbf{t}_j = \mathbf{Z}\mathbf{w}_j + \mathbf{t}_j^e, \\
& \mathbf{f}_j = t_a \mathbf{v}_1 + t_b \mathbf{v}_2 + t_c \mathbf{v}_3 + \left(h_1 \mathbf{M}_1 + h_2 \mathbf{M}_2 + h_3 \mathbf{M}_3\right) \mathbf{z}_j + \mathbf{N}\mathbf{t}_j, \\
& \mathbf{f}_j \geq \mathbf{0}, \quad \mathbf{z}_j \geq \mathbf{0}, \quad \mathbf{f}_j^T \mathbf{z}_j = 0, \\
& p_j^c = p_j^e + \mathbf{r}^T \mathbf{w}_j, \\
& t_c \geq t_b \geq t_a, \\
& \textit{bounds on} (t_a, t_b, t_c, h_1, h_2, h_3)
\end{aligned}
\tag{11}
$$

Again, constraints include bounds on the parameters as well as the inequality relations related to the tensile strength and breakpoint strengths. Notice that in the formulation of both the two-branch and three-branch softening laws, a convex-concave combination of softening behaviour is allowed.

The parameter identification problem, expressed generally as the constrained optimisation problem (9), belongs to a special class of problems in MPEC (Luo *et al.*, [28]) for which the equilibrium constraints are complementarity conditions. Because of the presence of complementarity constraints the optimization problem is a very difficult problem. It is well-known that MPECs fail to satisfy standard constraint qualifications such as the Mangasarian-Fromovitch Constraint Qualification (MFCQ). Violation of this constraint qualification is essentially synonymous with numerical instability of the feasible set and hence finding a solution to the problem becomes challenging.

The idea that an MPEC is simply a nonlinear program (Bard, [2]; Luo *et al.*, [28]) generalised to include some complementarity constraints led to the investigation of the applicability of NLP-based algorithms for the solution of the identification problem. A key strategy proposed

for the solution of MPEC (9) is through reformulation where NLP techniques can be applied. Since the major source of difficulty in MPECs lies with the complementarity constraints, the idea then is to eliminate or replace these constraints such that a solution to the reformulated problem is a solution to the MPEC. The development of suitable NLP-based algorithms capable of solving the challenging identification problem was addressed in the Ph.D. Dissertation by Que [34].

4. ENTROPIC REGULARIZATION AND COMPUTATIONAL RESULTS

The use of smoothing techniques in the area of complementarity problems has received renewed interests lately (Chen and Mangasarian, [14]; Chen and Harker, [13]; Gabriel and Moré, [22]). Studies have shown that smoothing techniques are promising tools for the solution of difficult mathematical problems. Tin-Loi and Que [39] have shown that a reformulation of the parameter identification problem (9) using a smoothing algorithm based on Fischer-Burmeister function yielded excellent results. In this paper, another smoothing function based on entropic regularization (Birbil *et al.*, [5]) is adopted for the solution of the MPEC (9).

A key idea in the smoothing algorithm is the replacement of the complementarity conditions $\mathbf{f}_j^T \mathbf{z}_j = 0$ by the set of equations

$$\phi_\mu (f_k, z_k) = 0, \quad \forall k, \tag{12}$$

where $k = 1, \ldots, 3n$ for two-branch laws and $k = 1, \ldots, 4n$ for three-branch laws. The function ϕ_μ has the property that $\phi_\mu (a, b) = 0$ if and only if $a \geq 0, b \geq 0, ab = \mu$. The particular ϕ_μ function (Birbil *et al.*, [5]) that is adopted in this work is:

$$\Phi_\mu (a, b) = -\frac{1}{\mu} \ln \left[exp(-a\mu) + exp(-b\mu) \right] \tag{13}$$

Denoting the functions $\phi_\mu (f_k, z_k)$ by $\Phi_\mu (\mathbf{f}, \mathbf{z})$, MPEC (9) can be reformulated as an NLP given by

$$\begin{array}{ll} \min\limits_{\forall j \in \mathbf{J}} & \omega \\ \textit{subject to} & \mathbf{t}_j = \mathbf{Z}\mathbf{w}_j + \mathbf{t}_j^e, \\ & \mathbf{f}_j \geq \mathbf{0}, \quad \mathbf{z}_j \geq \mathbf{0}, \quad \Phi_\mu (\mathbf{f}_j, \mathbf{z}_j) = \mathbf{0}, \\ & p_j^c = p_j^e + \mathbf{r}^T \mathbf{w}_j, \\ & \textit{other constraints} \end{array} \tag{14}$$

The algorithm proceeds by solving a series of nonlinear programs (or inner iterations), each represented by NLP (14), for increasing values of the smoothing parameter μ (or after each major iteration) until the desired complementarity tolerance has been met.

It must be noted that although the nonnegativity constraints $\mathbf{f}_j \geq \mathbf{0}$ and $\mathbf{z}_j \geq \mathbf{0}$ are strictly not required in the NLP (14), including them as constraints is beneficial in practice as their inclusion tend to speed up convergence as well as to increase numerical stability. It must be emphasised that the initial value of μ and its increase for each major iteration are problem dependent. An initial value of μ ranging from 1.0 to 5.0 for two-branch laws and 5.0 to 10.0 for

three-branch laws and the increase kept at a factor of 2.0 to 3.0 can yield good results in the identification problem. Too large an initial value may not provide a solution to the nonlinear program while too small a value may lead to a much more ill-conditioned initial NLP.

To test the applicability of the smoothing algorithm based on the smoothing function (13), actual test data are used. The General Algebraic Modelling System or GAMS (Brooke *et al.*, [9]) using version 2.5 with CONOPT2 (Drud, [18]) as solver is used to solve the reformulated MPEC. The identified parameters are then used as inputs to solve the MCP (8) using PATH (Dirkse and Ferris, [17]) which, in turn, enables one to obtain the predicted load - displacement $(p-u)$ curve. The predicted $p-u$ curve is then compared to actual data set. All runs are implemented using a Pentium 3 computer running at 850 MHz under Windows NT.

The first data set is obtained from a notched three-point bend test (Bolzon *et al.*, [8]) of a polymeric composite specimen made of an epoxy matrix with silicon micro-spherical hollow inclusions. The known properties of the tested specimen are $E = 3707$ MPa and $v = 0.39$. For the two-zone BEM modelling of the structural model, a total of 158 quadratic elements were used in the discretization where 15 elements (or 31 node pairs) were located at the interface.

Although all of the 48 recorded $p-u$ points can be used for the identification problem, sufficient information regarding the fracture behaviour of the specimen can be drawn using only 32 data points. Some preliminary computational results indicate that there is no significant gain in the accuracy of the identified fracture parameters when using all the recorded data points instead of the 32 subset points. There is however significant gain in computational cost when using only a subset of the $p-u$ data set as compared to the 48 recorded data points.

It must be noted that the points in the adopted $p-u$ data set are chosen such that they are reasonably equally spaced. This distribution has a regularization effect which reduces ill-conditioning of the data since clustering of data points is avoided. This is especially relevant for experimental observations where, typically, the recorded points contain noise and clustering. Computational experience indicates that this distribution scheme is particularly suitable for the parameter identification problem considered in this work.

The second data set is obtained from a wedge splitting test of normal strength concrete specimen (Denarié *et al.*, [16]). The specimen has the following recorded material properties: $E = 25200$ MPa and $v = 0.2$. The boundary element discretization of the structure consists of a total of 192 isoparametric quadratic elements, of which 17 pairs of elements (or 35 node pairs) are located along the potential crack interface. Although 128 $p-u$ points are recorded, these are very much clustered as Figure 5 indicates. Again, 32 reasonably spaced data points were chosen for the identification problem. This number is not only sufficient to describe satisfactorily the recorded experimental response, but also, being distinct points, reduced ill-conditioning.

The third data set is obtained from a notched three-point bend test (Olsen, [31]) of a normal strength concrete with material properties: $E = 26110$ MPa and $v = 0.2$. The dimensions of the structure is shown in Figure 6. The structural modelling of the specimen is carried out using a two-zone BEM discretisation. Each zone is discretised using a total of 121 isoparametric quadratic elements. At the potential crack interface, 18 pairs of quadratic elements (or 37 node pairs) are used. For this data set, the $p-u$ points are obtained by digitizing the reported $p-u$ curve in the literature. 32 $p-u$ point data set is also used for parameter identification.

Table I shows the identified parameters for a two-branch law. Also shown are the computed real error $\hat{\omega}$ and running time t in seconds. Starting value of the parameter μ for the first, second and third data sets are 5, 1 and 1 respectively. The parameter is then increased respectively by a factor of 2, 3 and 2 for the first, second and third data sets. Predicted $p-u$ curve for

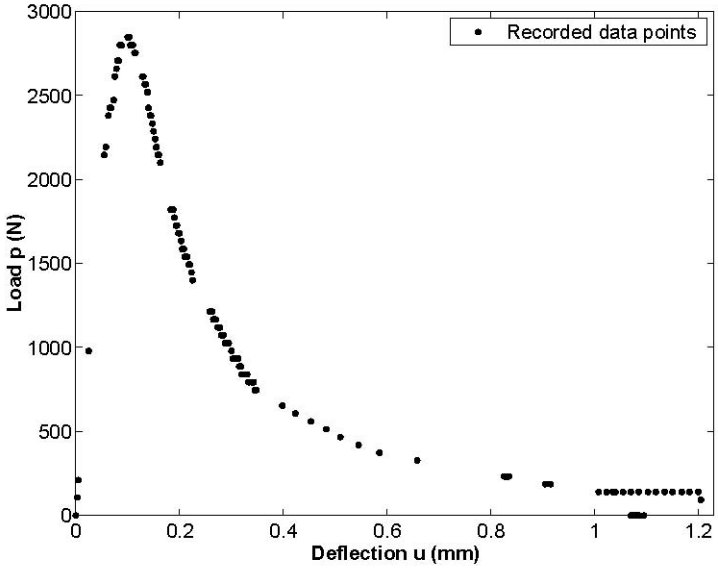

Figure 5. Plot of the 128 recorded data points of the LMC/EPFL wedge splitting test.

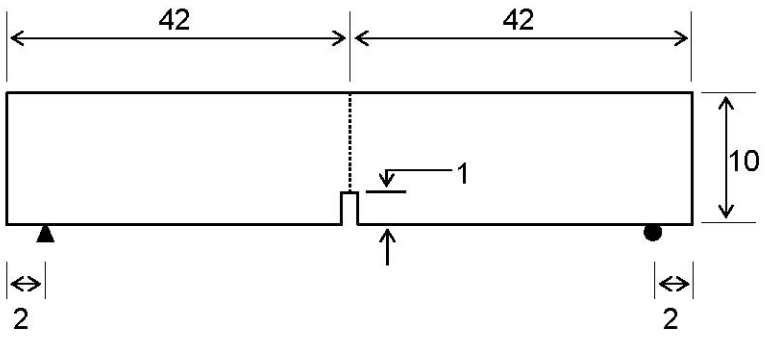

Figure 6. Dimensions for the structural model of data set 3.

each of the data sets are shown in Figures 7 to 9. The figures indicate that good agreement is achieved between the actual and predicted $p-u$ curves. Results also compare well with other reported NLP techniques (Tin-Loi and Que, [40]).

Results of the parameter identification problem using the three-branch law is shown in

Data	t_b	t_c	h_1	h_2	$\hat{\omega}$	t
1	2.643	11.214	332.279	44.547	11.960	1453
2	0.678	3.430	93.603	4.791	19.682	1342
3	0.544	2.481	48.377	3.026	15.002	593

Table I. Identification results for the two-branch law.

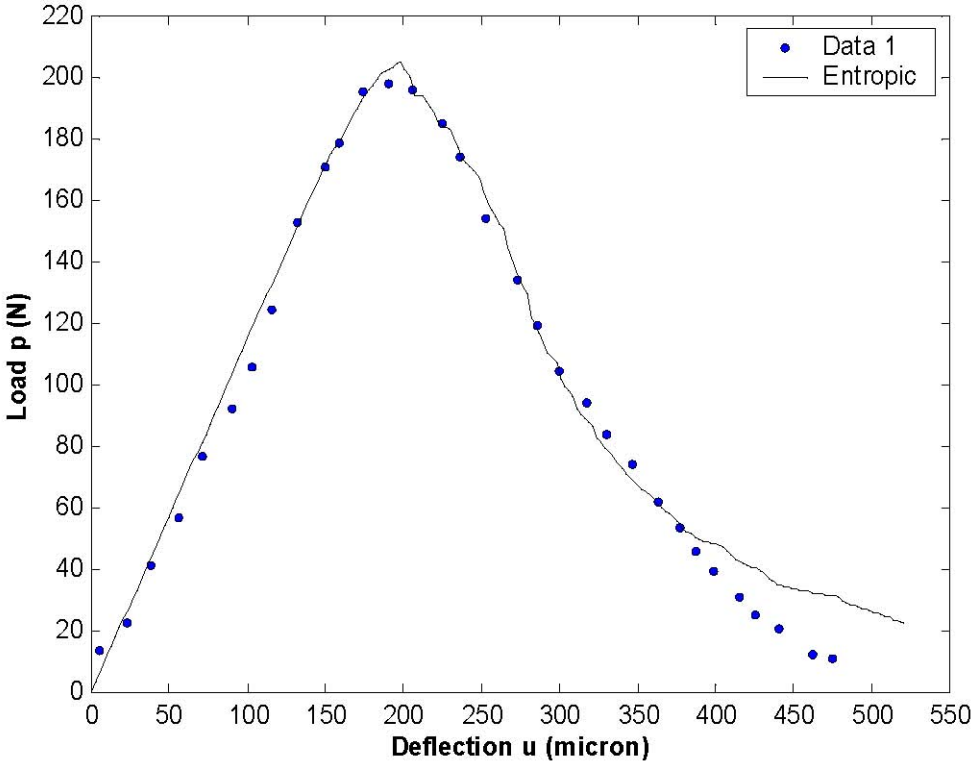

Figure 7. Data 1: Identified vs experimental $p-u$ curves using two-branch softening law.

Table II. For the data sets considered, the starting parameter μ is 10, 5 and 5 for the first, second and third data sets, respectively. As compared to the two-branch law, a higher starting value of μ seems to yield better results for the three-branch law. A factor of increase of 2 is used for each run of the NLP for all the data sets.

As in the two-branch law, a comparison of the experimental and predicted $p-u$ curves (Figures 10 to 12) shows excellent agreement. It is worth noting though that for the first data, the computed error is actually bigger for the three-branch law than that of the two-branch law. This may indicate that the solution may have converged prematurely for the reason that the identification problem considered is a highly nonconvex problem.

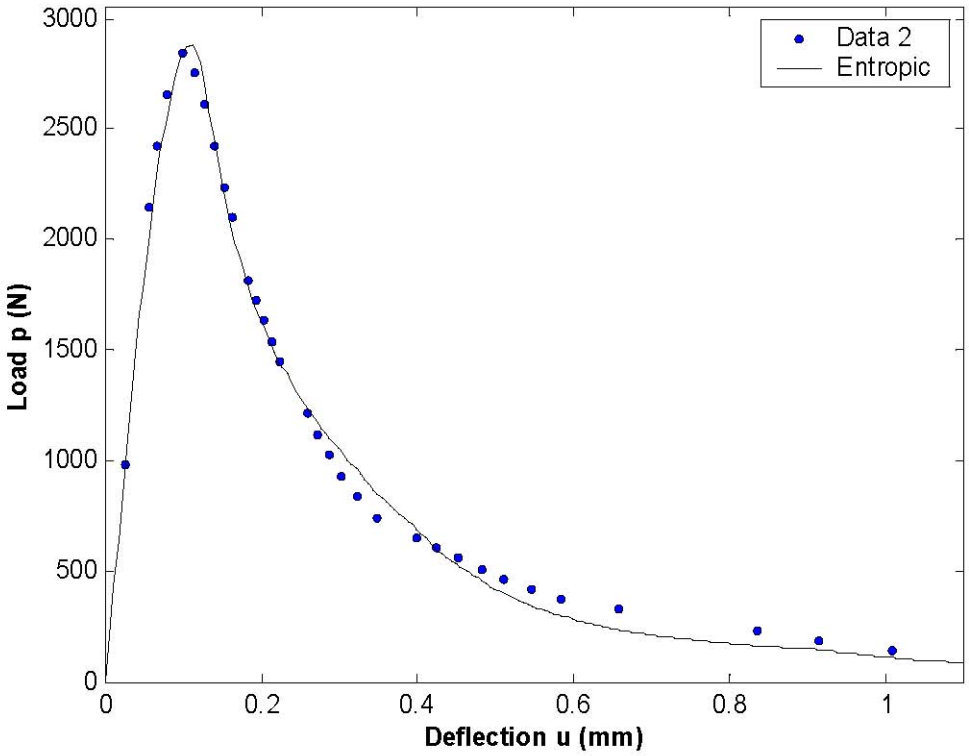

Figure 8. Data 2: Identified vs experimental $p - u$ curves using two-branch softening law.

Data	t_a	t_b	t_c	h_1	h_2	h_3	$\hat{\omega}$	t
1	0.564	2.786	10.949	314.755	52.948	18.846	17.570	2567
2	0.248	1.012	4.073	155.378	12.101	1.146	7.409	1589
3	0.423	1.329	3.279	141.707	19.148	2.464	10.939	1640

Table II. Identification results for the three-branch law.

Although the use of more softening branches may yield better agreement with the experimental data, it may not be practical as the run time can increase significantly. As has already been mentioned, for most practical purposes, a two-branch law may suffice to provide a good picture of the fracture behaviour of quasibrittle materials such as concrete. Comparing the identified tensile strengths of the materials, the use of a two-branch softening law often yields a more conservative result than that of the three-branch softening law.

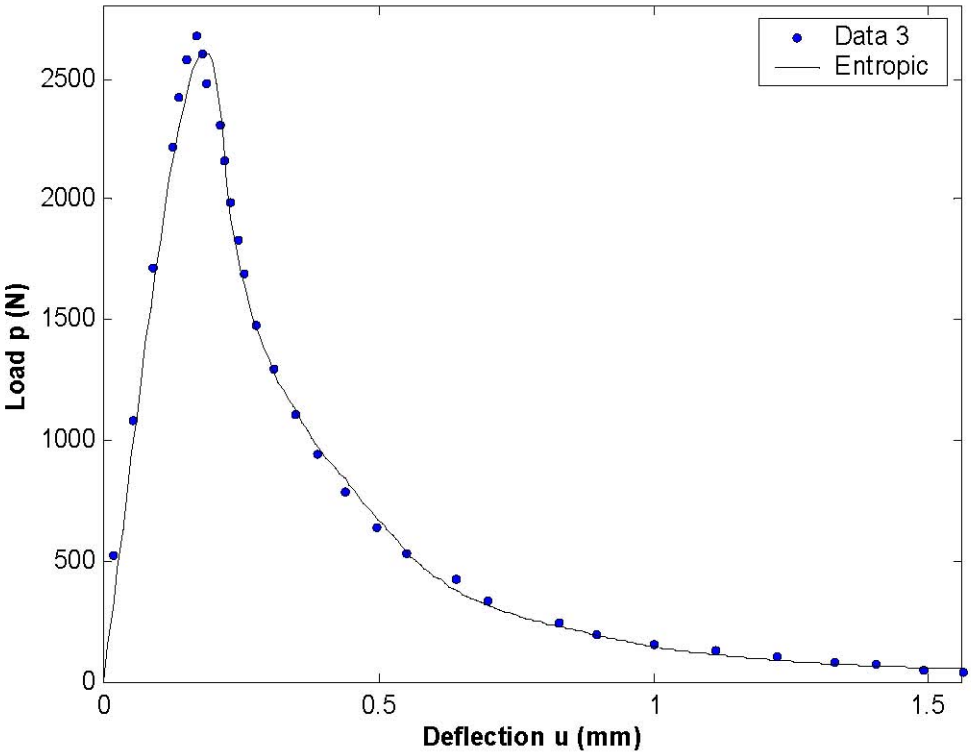

Figure 9. Data 3: Identified vs experimental $p - u$ curves using two-branch softening law.

5. CONCLUDING REMARKS

A smoothing technique based on entropic regularization is employed in the identification of the fracture parameters of the cohesive crack model. Results suggest that this approach compare well with other NLP techniques used in the identification problem (Tin-Loi and Que, [40]). However, the success of this smoothing function in the reformulation of the MPEC as NLP depends, to a large extent, on the goodness of the starting initial value as well as its eventual increase. The use of the entropic regularization function, in the context of the smoothing algorithm for parameter identification, as considered in this paper, does not seem to be as robust as that of the Fischer-Burmeister function (Kanzow, [27]) as reported in Tin-Loi and Que [40].

REFERENCES

1. Alvaredo, A.M. and Torrent, R.J. (1987) The effect of the shape of the strain-softening diagram on the bearing capacity of concrete beams, *Materials and Structures*, **20**, 448-454.

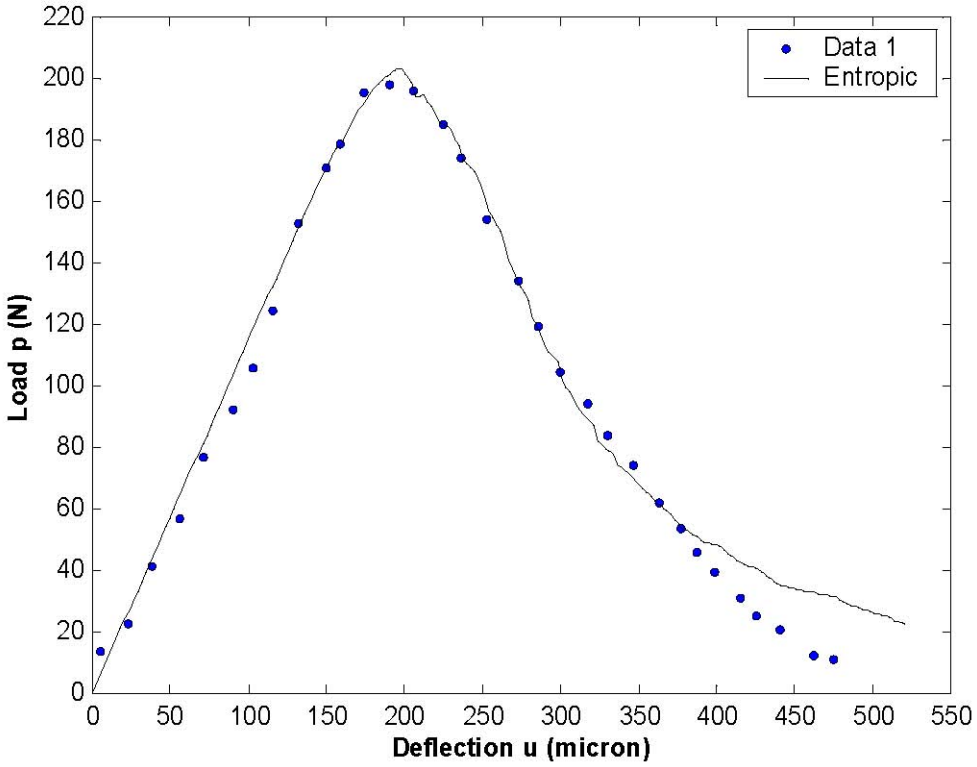

Figure 10. Data 1: Identified vs experimental $p - u$ curves using three-branch softening law.

2. Bard, J.F. (1991) Some properties of the bilevel programming problem, *Journal of Optimization Theory and Applications*, **68**, 371-378.
3. Barenblatt, G.I. (1962) The mathematical theory of equilibrium cracks in brittle fracture, *Advances in Applied Mechanics*, **7**, 55-129.
4. Bažant, Z. P. and Planas J. *Fracture and Size Effect in Concrete and Other Quasibrittle Materials* CRC Press Boca Raton (1998)
5. Birbil, S.I., Fang, S-C and Han, J. (2005) An entropic regularization approach for mathematical programs with equilibrium constraints, *Computers and Operations Research*, **31**, 2249-2262.
6. Bolzon, G. and Maier, G. (1998) Identification of cohesive crack models for concrete on the basis of three-point bending tests, In: *Computational Modelling of Concrete Structures* (Eds. de Borst, R., Bicanic, N., Mang, H. and Meschke, G.), Balkema, Rotterdam, 301-310.
7. Bolzon, G., Maier, G. and Novati, G. (1994) Some aspects of quasi-brittle fracture analysis as a linear complementarity problem, *Fracture and Damage in Quasibrittle Structures* (Eds. Bažant, Z.P., Bittnar, Z., Jirásek, M. and Mazars, J.), E&FN Spon, London, 159-174.
8. Bolzon, G., Maier, G. and Tin-Loi, F. (1997) On multiplicity of solutions in quasi-brittle fracture computations, *Computational Mechanics*, **19**, 511-516.
9. Brooke, A., Kendrick, D., Meeraus, A. and Raman, R. (1998) *GAMS: A User's Guide*, GAMS Development Corporation, Washington, DC 2007.
10. Carpinteri, A. and Massabò, R. (1997) Reversal in Failure Scaling Transition of Fibrous Composites, *Journal of Engineering Mechanics-ASCE*, **123**, 107-114.

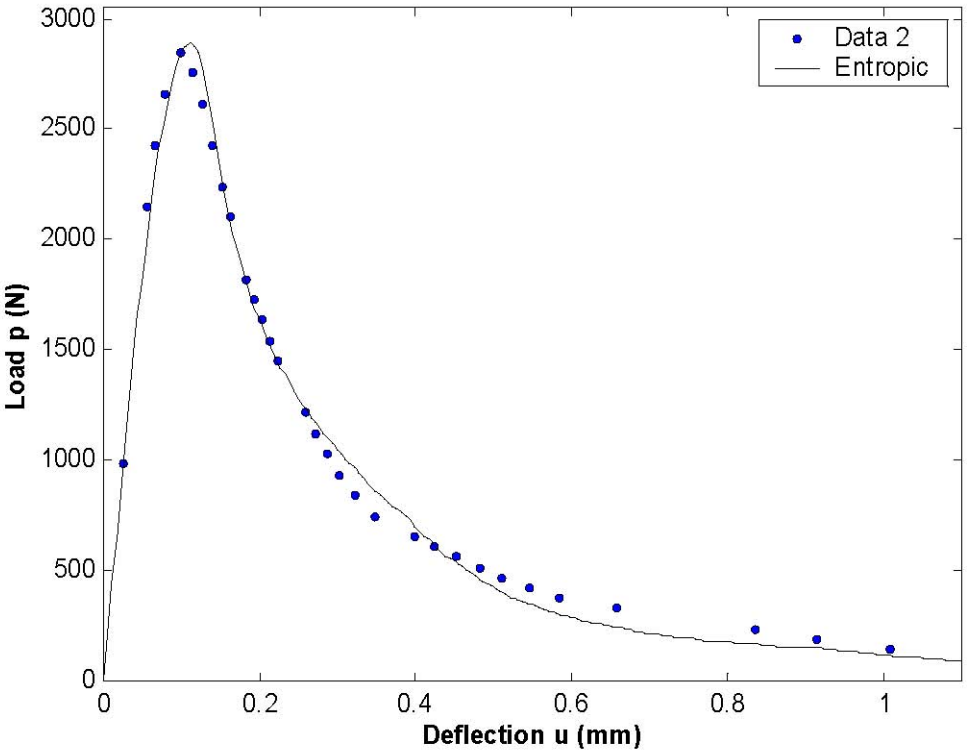

Figure 11. Data 2: Identified vs experimental $p - u$ curves using three-branch softening law.

11. Cattaneo, S. and Rosati, G. (1999) Effect of different boundary conditions in direct tensile tests: experimental results, *Magazine of Concrete Research*, **51**, 365-374.
12. Cen, Z. and Maier, G. (1992) Bifurcations and instabilities in fracture of cohesive-softening structures: a boundary element analysis, *Fatigue and Fracture of Engineering Materials and Structures*, **15**, 911-928.
13. Chen, B.T. and Harker, P.T. (1997) Smooth approximations to nonlinear complementarity problems, *SIAM Journal on Optimization*, **7**, 403-420.
14. Chen, C. and Mangasarian, O.L. (1996) Class of smoothing functions for nonlinear and mixed complementarity problems, *Computational Optimization and Applications*, **5**, 97-138
15. Cottle, R.W., Pang, J.S. and Stone, R.E. (1992) *The Linear Complementarity Problem*, Academic Press, Boston.
16. Denarié, E., Saouma, V.E., Iocco, A. and Varelas, D. (2001) Concrete fracture process zone characterization with fiber optics, *Journal of Engineering Mechanics-ASCE*, **127**, 494-502.
17. Dirkse, S.P. and Ferris, M.C. (1995) The PATH solver: a non-monotone stabilization scheme for mixed complementarity problems, *Optimization Methods and Software*, **5**, 123-156.
18. Drud, A.S. (1994) CONOPT - A large scale GRG code, *ORSA Journal on Computing*, **6**, 207-216.
19. Dugdale, D.S. (1960) Yielding of steel sheets containing slits, *Journal of the Mechanics and Physics of Solids*, **8**, 100-104.
20. Fang, S-C and Wu, S-Y (1996) Solving min-max problems and linear semi-infinite programs, *Computers and Mathematics with Applications*, **32**, 87-93.
21. Foote, R.M.L., Mai, Y.-W. and Cotterell, B. (1986) Crack growth resistance curves in strain-softening materials, *Journal of the Mechanics and Physics of Solids*, **34**, 593-607.

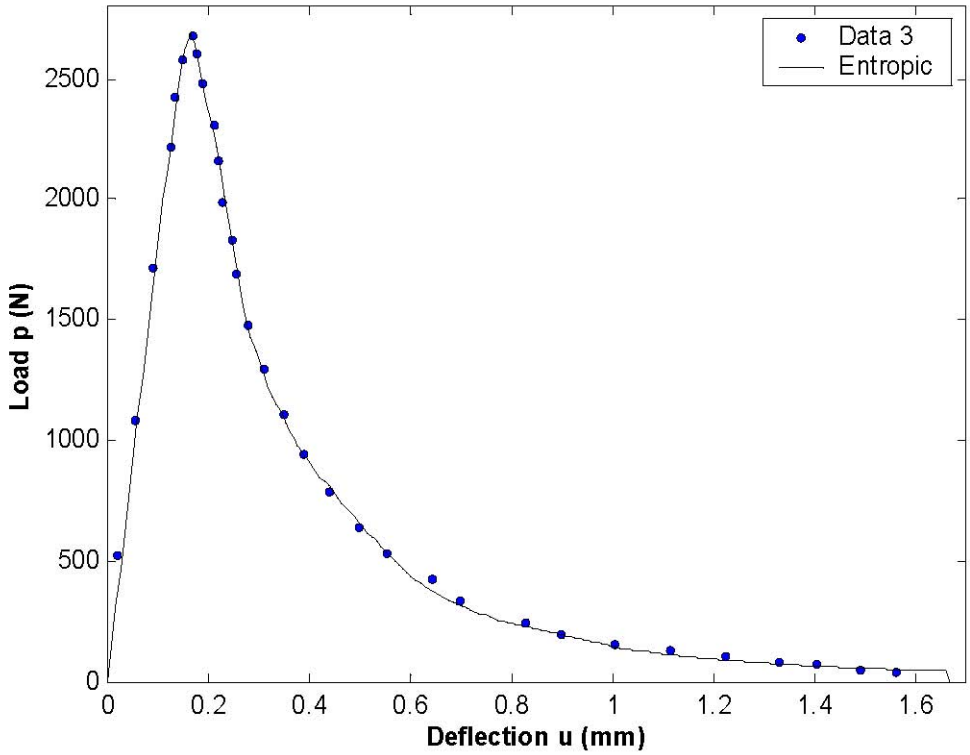

Figure 12. Data 3: Identified vs experimental $p - u$ curves using three-branch softening law.

22. Gabriel, S.A. and Moré, J.J. (1997) Smoothing of mixed complementarity problems, In: C*omplementarity and Variational Problems: State of the Art* (Eds. Ferris, M.C. and Pang, J.S.), SIAM Publications, Philadelphia, 105-116.
23. Guinea, G.V., Elices, M. and Planas, J. (1997) On the initial shape of the softening function of cohesive materials, *International Journal of Fracture*, **87**, 139-149.
24. Hillerborg, A., Modéer, M. and Petersson, P.E. (1976) Analysis of crack formation and crack growth in concrete by means of fracture mechanics and finite elements, *Cement and Concrete Research*, **6**, 773-782.
25. Hordijk, D.A., Reinhardt, H.W. and Cornelissen, H.A.W. (1987) Fracture mechanics parameters of concrete from uniaxial tensile tests as influenced by specimen length, In: *Fracture of Concrete and Rock, SEM-RILEM Conference* Houston, 138-149.
26. Hu, X.-Z. and Mai, Y.-W. (1992) Crack-bridging analysis for alumina ceramics under monotonic and cyclic loading, *Journal of the American Ceramic Society*, **75**, 848-853.
27. Kanzow, C. (1996) Some noninterior continuation methods for linear complementarity problems, *SIAM Journal on Matrix Analysis and Applications*, **17**, 851-868.
28. Luo, Z.Q., Pang, J.S. and Ralph, D. (1996) *Mathematical Programs with Equilibrium Constraints*, Cambridge University Press, Cambridge, New York.
29. Maier, G. and Frangi, A. (1998) Symmetric boundary element method for "discrete" crack modelling of fracture processes, *Computer Assisted Mechanics and Engineering Sciences*, **5**, 201-226.
30. Mihashi, H. and Nomura, N. (1996) Correlation between characteristics of fracture process zone and tension-softening properties of concrete, *Nuclear Engineering and Design*, **165**, 359-376.
31. Olsen, D.H. (1998) *Concrete fracture and crack growth: a fracture mechanics approach*, Report No. 42, Series R, Department of Structural Engineering and Materials, Technical University of Denmark, Denmark.

32. Petersson, P.E. (1981) Crack Growth and Development of Fracture Zones in Plain Concrete and Similar Materials, Report TVBM-1006, Division of Building Materials, Lund Institute of Technology, Lund, Sweden.
33. Planas, J. and Elices, M. (1991) Nonlinear fracture of cohesive materials, International Journal of Fracture, **51**, 139-157.
34. Que, N.S. (2003) Identification of Cohesive Crack Fracture Parameters Using Mathematical Programming, Ph.D. Dissertation, University of New South Wales, Sydney, Australia.
35. Que, N.S. and Tin-Loi, F. (2002) Numerical evaluation of cohesive fracture parameters from a wedge splitting test, *Engineering Fracture Mechanics*, **69**, 1269-1286.
36. Reinhardt, H.W., Cornelissen, H.A.W. and Hordijk, D.A. (1986) Tensile tests and failure analysis of concrete, *Journal of Structural Engineering - ASCE*, **112**, 2462-2477.
37. Reinhardt, H.W. and Xu, S.L. (1999) Crack extension resistance based on the cohesive force in concrete, *Engineering Fracture Mechanics*, **64**, 563-587.
38. Roelfstra, P.E. and Wittmann, F.H. (1986) Numerical method to link strain softening with failure of concrete, In: *Fracture Toughness and Fracture Energy of Concrete* (Ed. Wittmann, F.H.), Elsevier, Amsterdam, 163-175.
39. Tin-Loi, F. and Que, N.S. (2001) Parameter identification of quasibrittle materials as a mathematical program with equilibrium constraints, *Computer Methods in Applied Mechanics and Engineering*, **190**, 5819-5836.
40. Tin-Loi, F. and Que, N.S. (2002) Nonlinear programming approaches for an inverse problem in quasibrittle fracture, *International Journal of Mechanical Sciences*, **44**, 843-858.
41. Tin-Loi, F. and Xia, S.H. (2001) Holonomic softening: models and analysis, *Mechanics of Structures and Machines*, **29**, 65-84.
42. Ulfkjær, J.P. and Brincker, R. (1993) Indirect determination of the $\sigma - w$ relation of HSC through three-point bending, In: Fracture and Damage of Concrete and Rock (Ed. Rossmanith, H.P.), E&FN Spon, London, 135-144.
43. van Mier, J.G.M. and van Vliet, M.R.A. (2002) Uniaxial tension test for the determination of fracture parameters of concrete: state of the art, *Engineering Fracture Mechanics*, **69**, 235-247.

